From Interstellar Clouds to Star-Forming Galaxies: Universal Processes?
Proceedings IAU Symposium No. 315, 2015
P. Jablonka, Ph. André & F. van der Tak, eds.

doi:10.1017/S1743921316007328

SCUBA2 observations of prestellar cores

Derek Ward-Thompson and Kate Pattle,
on behalf of the JCMT and Herschel-SPIRE Gould Belt Consortia

Jeremiah Horrocks Institute, University of Central Lancashire,
Preston PR1 2HE, United Kingdom
email: dward-thompson@uclan.ac.uk

Abstract. We show data from the SCUBA2 camera on JCMT, of molecular clouds. We focus on starless cores within the clouds. We present data of the Taurus region and show how the environment is affecting some cores' appearance in this region. We compare the SCUBA2 data with Herschel data and discuss the sensitivity of SCUBA2 to surface brightness in the sub-millimetre. We show how this leads to its ability to pick out the densest cores at a given temperature. Hence SCUBA2 preferentially picks out gravitationally bound pre-stellar cores. We discuss the effects of the magnetic field, and how this lends support to a model for the formation and evolution of cores in filamentary molecular clouds.

Keywords. stars: formation – ISM: clouds – ISM: individual objects: L1495 – submillimeter: ISM

1. Introduction

Stars form in dense cores in molecular clouds. Exactly how these cores form is still a matter of debate (e.g. André *et al.*, 2014). Cores which do not contain any stars or newly-formed protostars are called starless cores. Those starless cores which are gravitationally bound are known as pre-stellar cores (Ward-Thompson *et al.*, 2007a; Di Francesco *et al.*, 2007). These pre-stellar cores then collapse to form Class 0 protostars (André *et al.*, 1993).

The James Clerk Maxwell Telescope (JCMT) Gould Belt Legacy Survey (GBLS) set out to map all nearby star-forming regions in various spectral lines, and also in the continuum at 850 μm with the Sub-mm Common-User Bolometer Array 2 (SCUBA2) camera (Ward-Thompson *et al.*, 2007b). This data-set can be used in comparison with the Herschel Gould Belt Survey (HGBS) at wavelengths from 70 to 500 μm (André *et al.*, 2010; Pattle *et al.*, 2015).

Cores are a significant stage in star formation. Recent work by the HGBS and the JCMT GBLS has led to new insight into core formation (André *et al.*, 2014). One of the goals of the GBLS was to catalogue and map all of the pre-stellar cores within about 0.5 kpc (Ward-Thompson *et al.*, 2007b). The mass function of cores can then be modelled onto the IMF of stars (Goodwin *et al.*, 2008).

2. Taurus

Figure 1 shows the L1495 region in Taurus (Ward-Thompson *et al.*, 2016). Five Herschel wavebands and one waveband from SCUBA2 are shown. A number of cores and filamentary structures can be seen. In particular a triangle-shaped arrangement of filaments can be seen just below centre of each image. The ubiquity of filaments is a feature seen in almost all of the Herschel data of star-forming regions (André *et al.*, 2010).

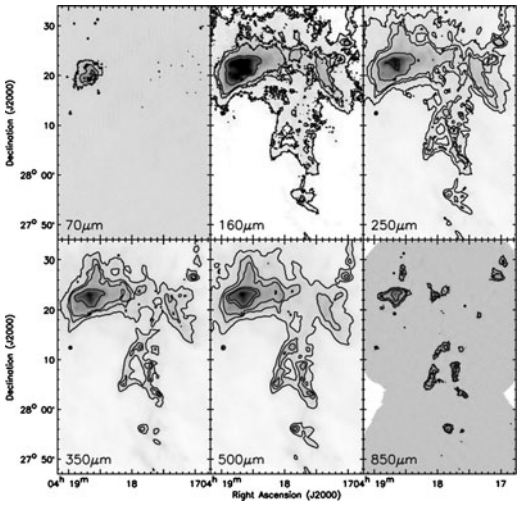

Figure 1. Herschel and SCUBA2 images of the L1495 molecular cloud in Taurus. Top row, left to right: 60, 170 and 250 μm respectively. Lower row, left to right: 350 and 500 μm (all from Herschel) and 850 μm (from SCUBA2) respectively. Note how SCUBA2 only detects some of the cores seen at the other wavelengths by Herschel (Ward-Thompson *et al.*, 2016).

The bright region towards the upper part of the image that is seen at most wavebands is the L1495A core, and is exactly coincident with L1495A-S. This lies at the head of a large, filamentary structure that is seen clearly in the Herschel data of the Taurus region (Marsh *et al.*, 2016). We measured a temperature gradient across this core, with the hotter material lying to the south (Ward-Thompson *et al.*, 2016).

There is a bright star, slightly to the south of L1495A-S, which is known as V892 Tau (IRAS04155+2812). This is a Herbig Ae/Be star, and it is clearly heating L1495A-S, which is otherwise starless, and causing the temperature gradient across the core. So we see that environment is affecting the appearance of some cores in the far-infrared and sub-mm. Similar effects were seen in cores in Cepheus (Nutter *et al.*, 2009; Pattle *et al.*, 2016). Note that only some of the cores visible in the Herschel images are seen in the SCUBA2 image. For example, the filament to the upper right in the Herschel images appears to Herschel as no different from the other filaments, but it is almost invisible in the SCUBA2 image.

Figure 2 shows a plot of density versus temperature for the starless cores in the L1495 region. The cores detected by SCUBA2 are indicated by black crosses. Those that are detected by Herschel are indicated by green crosses. The cores detected by SCUBA2 all lie in the upper part of this plot (Ward-Thompson *et al.*, 2016). However, note that both sets of cores occupy a similar range of temperatures.

Figure 3 shows a plot of mass versus deconvolved full-width at half-maximum (FWHM) size for the starless cores in the L1495 region. The cores detected by SCUBA2 are indicated by black points. Those that are detected by Herschel are indicated by green points. The cores detected by SCUBA2 all lie in the upper part of this plot (Ward-Thompson *et al.*, 2016). However, both set of cores occupy a similar range of sizes.

Figures 2 and 3 taken together would appear to indicate that SCUBA2 is only sensitive to the densest cores, or to the most massive cores for a given size, whereas Herschel sees more of the cores (Ward-Thompson *et al.*, 2016). This can be understood in terms of a surface brightness effect in the SCUBA2 data. For a given, relatively narrow, range of temperatures, such as is observed in starless cores, SCUBA2 surface brightness traces

https://doi.org/10.1017/S1743921316007328 Published online by Cambridge University Press

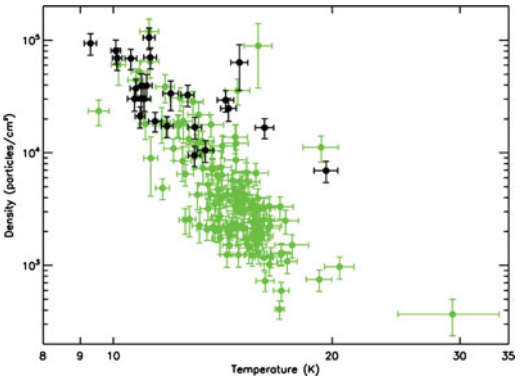

Figure 2. Density plotted against temperature for Herschel (grey crosses) and SCUBA2 (black crosses) data of starless cores. Note how both data-sets span a similar range of temperatures, but that the SCUBA2 cores only occupy the higher density parts of the plot (Ward-Thompson *et al.*, 2016).

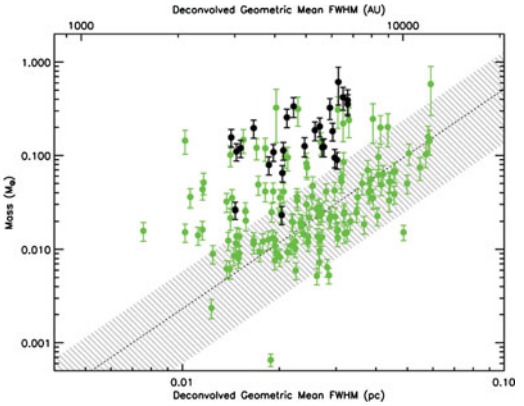

Figure 3. Mass plotted against deconvolved FWHM for Herschel (grey crosses) and SCUBA2 (black crosses) data of starless cores. Note how both data-sets span a similar range of FWHM size, but that the SCUBA2 cores only occupy the higher mass parts of the plot (Ward-Thompson *et al.*, 2016).

column density. Furthermore, for normally non-elongated structures, such as starless cores, column density effectively traces volume density. Hence the surface brightness of a starless core seen in a SCUBA2 image traces the density of that core. All of this implies that SCUBA2 will preferentially detect the densest cores – i.e. those closest to gravitational collapse – pre-stellar cores (Ward-Thompson *et al.*, 2016).

3. Magnetic fields

The magnetic field direction (in the plane of the sky) in a molecular cloud can be inferred from sub-mm dust continuum polarization measurements. Figure 4 shows results from the Ballon-borne Large Aperture Sub-mm Telescope Polarimeter (BLASTPol) of a filamentary structure in the Lupus molecular cloud (Matthews *et al.*, 2014). The curved line traces the axis of the filament. The vectors trace the direction of the magnetic field inferred from the polarization measurements. Note how the B-field lies largely perpendicular to the direction of the filament axis (Matthews *et al.*, 2014).

Observations such as these have led to a new model being proposed for core formation (André *et al.*, 2014). In this new scenario, material is funnelled onto filaments by the

https://doi.org/10.1017/S1743921316007328 Published online by Cambridge University Press

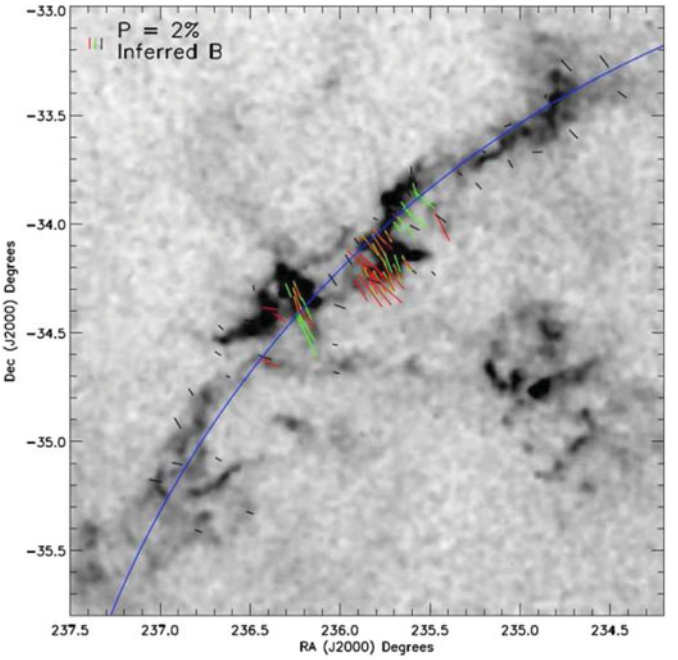

Figure 4. BLASTPol B-field vectors superposed on a sub-mm image of the Lupus molecular cloud. The vectors trace the direction of the magnetic field. The curved line traces the axis of the filament. Note how the B-field lies largely perpendicular to the direction of the filament axis (Matthews *et al.*, 2014). *(A color version of this figure is available online.)*

magnetic field (Palmeirim *et al.*, 2013). Dense parts of the filaments form cores by accreting further matter along the filaments. The filaments accrete mass until they exceed the critical mass per unit length against gravitational instability (Kawachi & Hanawa 1998). At this point they collapse under self-gravity to form proto-stellar cores. Herschel observed that roughly two-thirds of cores form in this manner (Könyves *et al.*, 2015).

References

André, P., Ward-Thompson, D., & Barsony, M. 1993, *ApJ* 406 122
André, P., Men'shchikov, A., Bontemps, S., *et al.* 2010, *A&A* 518 102
André, P., Di Francesco, J., Ward-Thompson, D., *et al.* 2014, *Protostars & Planets VI* p. 27
Di Francesco, J., Evans, N. J. II, Caselli, P., *et al.* 2007, *Protostars & Planets V* p. 17
Goodwin, S. P., Nutter, D., Kroupa, P., *et al.* 2008, *A&A* 477 823
Kawachi, T. & Hanawa, T., 1998, *PASJ* 50 577
Könyves, V., André, P., Mensh'chikov A., *et al.* 2015, *A&A*, 584, A91
Marsh, K. M., Kirk, J. M., André, P., *et al.* 2016, *MNRAS* submitted
Matthews, T. G., Ade, P. A. R., Angilè, F. E., *et al.* 2014, *ApJ* 784 116
Nutter, D., Stamatellos, D., Ward-Thompson, D. 2009 *MNRAS* 396 1851
Palmeirim, P., André, P. Kirk, J. M., Ward-Thompson, D., *et al.* 2013, *A&A* 550 A38
Pattle, K., Ward-Thompson, D., Kirk, J. M., White, G. J. *et al.* 2015, *MNRAS* 450 1094
Pattle, K., Ward-Thompson, D., Keown, J., *et al.* 2016 *MNRAS* in prep.
Ward-Thompson, D., André, P., Crutcher, R., *et al.* 2007, *Protostars & Planets V* p.33
Ward-Thompson, D., Di Francesco, J., Hatchell, J., *et al.* 2007, *PASP* 119 855
Ward-Thompson, D., Pattle, K., Kirk, J. M. *et al.* 2016, *MNRAS* in prep.

https://doi.org/10.1017/S1743921316007328 Published online by Cambridge University Press